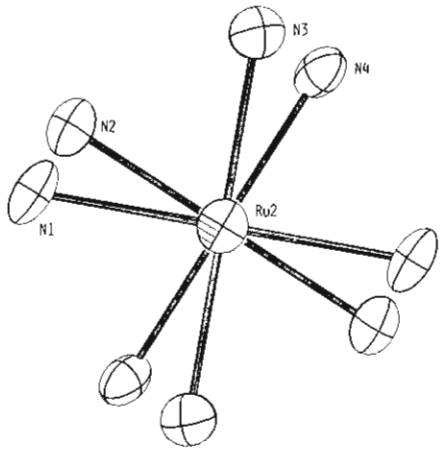

Figure 4. View down the Ru(1)–Ru(2) axis in $Ru_2Cl(PhNpy)_4$ showing the conformation of the eight equatorial atoms coordinated to the diruthenium unit.

$PhNpy^-$ ion tends to reside primarily on the amine nitrogen atom N_{am}, we might expect the Ru–N_{am} bond length to be shorter than the Ru–N_{py} distances, and this is indeed the case. The Ru–N_{am} distances are about 0.08 Å shorter than the Ru–N_{py} distances. In the $M_2(PhNpy)_4$ molecules[10] (M = Mo, W) there was also a difference in the same direction, but it was very much smaller, viz., about 0.02 Å. It would thus appear that some factor other than charge distribution in the ligand must be at work. Probably, the lack of an axial ligand on Ru(2) permits the closer approach of the four equatorial ligands.

The unusual arrangement of ligands in **9** engenders rather large torsion angles about the Ru–Ru bond, as shown in Figure 4 and presented in Table VI. The torsional angles, N(2)–Ru(1)–Ru(2)–N(1) and N(4)–Ru(1)–Ru(2)–N(3), are 22.8 and 22.6°, respectively. In the previously known complexes of 2-anilinopyridine, which are all of the structural type **3**, no significant twists were seen.

Concluding Comments. These two new examples of the totally polar mode of coordination of unsymmetrical bidentate ligands across M–M bonds demonstrate that such arrangements are probably not as rare or unlikely as had been assumed only a little while ago. The question of what factors favor the occurrence of such an arrangement is now of greater importance since the phenomenon is now less of an oddity. A combination of both steric and bonding factors would seem to be operative in all cases.

Perhaps the most straightforward case is present in compound **9**. If there is a strong tendency for the Ru_2^{5+} core to have a Cl^- ion coordinated at one axial position, then once this is done there is a strong steric factor disfavoring the coordination of a Ph–N– nitrogen atom to the same metal atom. Since there is room for all four phenyl groups at the other end, provided some torsion about the Ru–Ru bond occurs, such an arrangement is adopted. In this way one very good axial Ru–Cl bond can be formed without a major penalty (since the Ru–Ru bond has no rotational barrier), whereas for a bridging ligand set of type **3** or **4** a strong Ru–Cl bond might not be possible at either end.

In the case of **8**, it seems that steric factors alone may favor the observed arrangement, but not very decisively. The axial bridging of the Hhp molecule, supported by the hydrogen bond, may well be a stabilizing factor. Its presence may then favor an orientation of the other three hp ligands that are not hydrogen bonded that keeps their bulky pyridine rings away from the axial Hhp molecule. However, there must also be some repulsive force between the C(*n*5)–H groups of these rings and the axial chlorine atom at the other end. The net result of this trade-off would not seem to be immediately obvious.

Finally, in the $M_2(fhp)_4THF$ molecules (M = Cr, Mo, W, Rh), the balance of steric forces would again seem to be a close one. With all fhp ligands directed one way, one metal atom can form one very good M–THF axial bond, whereas, if two fhp bonds were directed each way, both ends of the M_2 unit might be sufficiently encumbered as to allow only very weak M–THF interactions.

Acknowledgment. We are grateful to the National Science Foundation for financial support.

Registry No. **8**, 94089-98-2; **9**, 94089-99-3; $Ru_2(O_2CCH_3)_4Cl$, 38833-34-0.

Supplementary Material Available: Details of the crystal structure determination and listings of angles, anisotropic thermal parameters, distances, and observed and calculated structure factors (46 pages). Ordering information is given on any current masthead page.

Contribution from the Department of Chemistry and Laboratory for Molecular Structure and Bonding, Texas A&M University, College Station, Texas 77843

$\delta \rightarrow \delta^*$ Transition Energies as a Function of δ-Bond Strength: An Extrapolative Assessment of the Ground-State Electron Correlation Energy

FRED L. CAMPBELL, III, F. ALBERT COTTON,* and GREGORY L. POWELL

Received May 25, 1984

The structural characterization of two partially staggered $Mo_2X_4(LL)_2$ compounds is reported, and their relevance to the relationship between $\delta \rightarrow \delta^*$ transition energy and torsional twist in quadruply bonded molybdenum dimers is discussed. A second crystallographic form of β-$Mo_2Cl_4(dmpe)_2$ has been subjected to X-ray crystallographic analysis and will be designated as β'-$Mo_2Cl_4(dmpe)_2$ (**1**). It crystallizes in space group $P4_22_12$ with $a = b = 12.124$ [5] Å, $c = 8.805$ (2) Å, $V = 1294$ (1) Å^3, and $Z = 2$. In addition, an analogous bromo compound, β-$Mo_2Br_4(dmpe)_2$ (**2**), has been prepared and characterized. It crystallizes in space group $P2_12_12_1$ with $a = 13.739$ (3) Å, $b = 13.774$ (3) Å, $c = 14.211$ (2) Å, $V = 2689$ (2) Å^3, and $Z = 4$. These two compounds together with eight others that have been previously studied structurally are used to examine the relationship between the energy of the $A_{1g} \rightarrow A_{2u}$ ($\delta \rightarrow \delta^*$) electronic transition and the strength of the δ bond. The latter is taken to be a linear function of cos (2χ), where χ is the angle of internal rotation away from the fully eclipsed conformation. The observed transition energies extrapolate to a value of $(11.8 \pm 0.3) \times 10^3$ cm^{-1} at cos (2χ) = 0. It is proposed that this "residual" energy can be attributed mainly to the difference between the correlation energies in the ground ($\sigma^2\pi^4\delta^2$) and excited ($\sigma^2\pi^4\delta\delta^*$) electron configurations. The extrapolated energy is close to those obtained in previous electronic structure calculations on $Mo_2Cl_8^{4-}$ and related systems.

Introduction

It has been noted[1,2] that the δ components of metal–metal bonds of order 3.5 and higher, especially those of order 4, where the δ-bonding orbital is doubly occupied, have interesting structural and spectroscopic properties. In compounds of the type $M_2X_4(LL)_2$, where LL is a bridging bidentate ligand such as an $R_2P(CH_2)_nPR_2$ type diphosphine, the steric requirements of the LL ligands introduce various angles of internal rotation, χ, away from the angle $\chi = 0$ that defines the precisely eclipsed conformation in which the δ-bond strength has its maximum value. These

(1) Cotton, F. A.; Walton, R. A. "Multiple Bonds Between Metal Atoms"; Wiley: New York, 1982; pp 390–402.
(2) Cotton, F. A. *Chem. Soc. Rev.* **1983**, *12*, 35.

0020-1669/85/1324-0177$01.50/0

Table I. Summary of Crystal Data, Data Collection Parameters, and Least-Squares Residuals for Compounds **1** and **2**

compd	β'-$Mo_2Cl_4(dmpe)_2$ (**1**)	β-$Mo_2Br_4(dmpe)_2$ (**2**)
formula	$Mo_2Cl_4P_4C_{12}H_{32}$	$Mo_2Br_4P_4C_{12}H_{32}$
fw	633.97	811.78
space group	$P4_22_12$	$P2_12_12_1$
syst abs	$h00$ ($h = 2n$), $00l$ ($l = 2n$)	$h00$ ($h = 2n$), $0k0$ ($k = 2n$), $00l$ ($l = 2n$)
a, Å	12.124 [5]	13.739 (3)
b, Å	$=a$	13.774 (3)
c, Å	8.805 (2)	14.211 (2)
V, Å^3	1294 (1)	2689 (2)
Z	2	4
d_{calcd}, g/cm^3	1.627	2.005
cryst size, mm	0.15 × 0.15 × 0.40	0.21 × 0.22 × 0.35
μ(Mo Kα), cm^{-1}	16.04	74.39
data collcn instrum	Enraf-Nonius CAD-4	
radiation (monochromated in incident beam)	Mo Kα	
orientation reflcns: no.; range (2θ), deg	25; 15–35	25; 16–37
temp, °C	25 (2)	
scan method	ω–2θ	
data collcn range (2θ), deg	5–50	
total no. of unique data	1188	2497
data with $F_o^2 > 3\sigma(F_o^2)$	781	1525
no. of parameters refined	53	199
transmissn factors: max, min	none	99.65, 66.98
R^a	0.0382	0.0389
$R_w{}^b$	0.0557	0.0451
quality-of-fit indicator[c]	1.453	1.165
largest shift/esd, final cycle	0.03	0.09
largest peak, e/Å^3	0.84	0.59

[a] $R = \Sigma||F_o| - |F_c||/\Sigma|F_o|$. [b] $R_w = [\Sigma w(|F_o| - |F_c|)^2/\Sigma w|F_o|^2]^{1/2}$; $w = 1/\sigma(|F_o|)^2$. [c] Quality of fit = $[\Sigma w(|F_o| - |F_c|)^2/(N_{observns} - N_{parameters})]^{1/2}$.

internal twists engender several interesting phenomena. They make the chromophore chiral, thus giving rise to CD and ORD spectra.[3] They also lead to a lengthening of the M–M distance because of the decreased contribution of the δ component to the total bond strength.[4] A third phenomenon forms the subject of this paper, namely, a decrease in the $\delta \rightarrow \delta^*$ transition energy as the δ bond is weakened. This effect, however, shows a more complicated dependence on the angle of rotation than might have been expected from a superficial analysis. We report here the full set of experimental results and offer an interpretation for the principal features of the functional dependence of the transition energy on cos (2χ), namely, nonlinearity and a nonzero intercept with the energy axis when cos (2χ) = 0.

Experimental Section

All manipulations were carried out under dry, air-free conditions with use of Schlenk and vacuum line techniques. Toluene and hexane were dried with potassium/benzophenone and distilled under nitrogen before use. 1,2-Bis(dimethylphosphino)ethane was purchased from Strem Chemicals, Inc., and used without further purification. *tert*-Butyl peroxide was obtained from Pfaltz and Bauer, Inc., and used as received. β-$Mo_2Cl_4(dmpe)_2$[4] was prepared according to the published procedure.

$Mo_2Br_4(PEt_3)_4$ was prepared by stirring a mixture of 3.33 g (7.78 mmol) of $Mo_2(O_2CCH_3)_4$, 6.4 mL of (43.9 mmol) PEt_3, and 5.6 mL of (42.4 mmol) Me_3SiBr in 60 mL of CH_2Cl_2 for 15 h and then refluxing this mixture for 3 h. After the mixture was cooled to room temperature, all except ca. 5 mL of the solvent was removed by vacuum distillation. Methanol (30 mL) was added and the resulting suspension stirred for 10 min. The purple product was collected by suction filtration, washed with 40 mL of water and 10 mL of ethanol, and dried in vacuo; yield 62%. Although this method of preparation is much more convenient than the previously reported procedures,[5,6] the product contains traces of $Mo_2(O_2CCH_3)$ even after repeated washing with water. Pure $Mo_2Br_4(PEt_3)_4$ may be obtained by dissolving the crude product in toluene, filtering through Celite, and removing the solvent by vacuum distillation.

Table II. Positional and Isotropic Equivalent Thermal Parameters for β'-$Mo_2Cl_4(dmpe)_2$ (**1**)[a,b]

atom	x	y	z	B,[a] Å^2
Mo	0.93677 (5)	0.937	1.000	4.31 (1)
Mo(2)	1.000	1.000	0.879 (3)	4.4 (4)[c]
Cl	0.8239 (2)	0.9494 (3)	0.7785 (3)	9.12 (8)
P	1.0489 (3)	0.7894 (2)	0.8694 (4)	8.08 (8)
C(1)	1.186 (1)	0.7700 (9)	0.946 (2)	15.7 (5)
C(2)	0.986 (2)	0.6512 (9)	0.894 (2)	13.2 (5)
C(3)	1.072 (1)	0.796 (1)	0.666 (1)	13.4 (5)

[a] Anisotropically refined atoms are given in the form of the isotropic equivalent thermal parameter defined as $^4/_3[a^2\beta_{11} + b^2\beta_{22} + c^2\beta_{33} + ab(\cos\gamma)\beta_{12} + ac(\cos\beta)\beta_{13} + bc(\cos\alpha)\beta_{23}]$. [b] Estimated standard deviations in the least significant digits are given in parentheses. Values for which no esd's appear were not refined. [c] Refined isotropically.

Table III. Positional and Isotropic Equivalent Thermal Parameters for β-$Mo_2Br_4(dmpe)_2$[a,b]

atom	x	y	z	B,[a] Å^2
Mo(1)	0.53747 (9)	0.53631 (9)	0.90939 (9)	2.69 (3)
Mo(2)	0.4754 (1)	0.4816 (1)	1.03928 (9)	2.95 (3)
Br(1)	0.6252 (1)	0.3981 (1)	0.8265 (1)	4.89 (4)
Br(2)	0.4970 (1)	0.7160 (1)	0.8935 (2)	5.31 (5)
Br(3)	0.3124 (1)	0.5656 (1)	1.0634 (1)	4.72 (4)
Br(4)	0.5913 (2)	0.3565 (2)	1.1102 (1)	6.55 (5)
P(1)	0.4005 (3)	0.5066 (3)	0.7931 (3)	3.5 (1)
P(2)	0.7046 (4)	0.5902 (4)	0.9640 (4)	5.6 (1)
P(3)	0.3765 (4)	0.3380 (3)	0.9790 (3)	4.2 (1)
P(4)	0.5441 (4)	0.6018 (4)	1.1579 (4)	6.0 (1)
C(11)	0.343 (1)	0.386 (1)	0.790 (1)	4.6 (4)
C(12)	0.444 (1)	0.513 (2)	0.671 (1)	6.5 (5)
C(13)	0.293 (1)	0.590 (1)	0.799 (1)	5.2 (5)
C(21)	0.713 (1)	0.673 (1)	1.066 (2)	7.7 (6)
C(22)	0.796 (1)	0.495 (2)	0.989 (2)	8.2 (7)
C(23)	0.763 (1)	0.663 (2)	0.871 (2)	10.0 (8)
C(31)	0.289 (1)	0.359 (1)	0.883 (1)	5.0 (5)
C(32)	0.442 (1)	0.227 (1)	0.941 (1)	6.0 (5)
C(33)	0.295 (2)	0.290 (1)	1.070 (1)	6.4 (5)
C(41)	0.678 (2)	0.628 (2)	1.159 (2)	10.9 (7)
C(42)	0.494 (1)	0.726 (1)	1.159 (1)	6.6 (5)
C(43)	0.523 (2)	0.557 (2)	1.279 (1)	10.8 (8)

[a] Anisotropically refined atoms are given in the form of the isotropic equivalent thermal parameter defined as $^4/_3[a^2\beta_{11} + b^2\beta_{22} + c^2\beta_{33} + ab(\cos\gamma)\beta_{12} + ac(\cos\beta)\beta_{13} + bc(\cos\alpha)\beta_{23}]$. [b] Estimated standard deviations in the least significant digits are given in parentheses.

Preparations. The New Form of β-$Mo_2Cl_4(dmpe)_2$ (1). A mixture of 0.70 g (1.1 mmol) of β-$Mo_2Cl_4(dmpe)_2$ and 0.30 mL (1.6 mmol) of *tert*-butyl peroxide was stirred and refluxed for 10 h in 35 mL of toluene. No reaction apparently occurred since the electronic absorption spectrum of the reaction solution in the visible region was identical with that of β-$Mo_2Cl_4(dmpe)_2$ dissolved in toluene. Crystals suitable for X-ray crystallography were grown by slightly reducing the volume of this "reaction" solution and cooling at −20 °C.

β-$Mo_2Br_4(dmpe)_2$ (2). This was accomplished with use of a procedure analogous to that previously employed in the preparation of β-$Mo_2Cl_4(dmpe)_2$.[4] A 7.0-mL portion (2.3 mmol of dmpe) of a 0.33 M solution of dmpe in toluene was added to a stirred solution of 1.00 g (1.02 mmol) of $Mo_2Br_4(PEt_3)_4$ in 65 mL of toluene. This mixture was refluxed for 20 h and then filtered through a medium frit. In order to obtain crystals, 5 mL of the filtrate was transferred to a Schlenk tube and layered with 20 mL of hexane. The volume of the remainder of the filtrate was reduced to ca. 10 mL, and hexane (40 mL) was added to precipitate the red-brown product in 82% yield. In contrast to the synthesis of the chloro analogue, none of the chelated (α) form of $Mo_2B_4(dmpe)_2$ was produced.

X-ray Crystallography. An Enraf-Nonius CAD-4 diffractometer equipped with Mo Kα radiation was used to collect data on crystals of compounds **1** and **2** at room temperature (25 ± 2 °C). The general

(3) Agaskar, P.; Cotton, F. A.; Fraser, I. F.; Peacock, R. D. *J. Am. Chem. Soc.* **1984**, *106*, 1851.
(4) Cotton, F. A.; Powell, G. L. *Inorg. Chem.* **1983**, *22*, 1507.
(5) San Filippo, J.; Sniadoch, H. J.; Grayson, R. L. *Inorg. Chem.* **1974**, *13*, 2121.
(6) Glicksman, H. D.; Hamer, A. D.; Smith, T. J.; Walton, R. A. *Inorg. Chem.* **1976**, *15*, 2205.

Table IV. Bond Distances (Å) and Angles (deg) for β'-$Mo_2Cl_4(dmpe)_2$ (1)

	Distances		
Mo-Mo′	2.168 (1)	C(1)-C(1)′	1.21 (3)
-Cl	2.387 (2)	Mo(2)-Mo(2)′	2.12 (4)
-P	2.522 (3)	-Mo	1.517 (14)
P-C(1)	1.815 (14)	-Cl	2.392 (8)
-C(2)	1.852 (12)	-P	2.622 (3)
-C(3)	1.818 (12)		
	Angles		
Mo′-Mo-Cl	111.09 (7)	C(1)-P-C(3)	103.3 (9)
-P	96.88 (8)	C(2)-P-C(3)	102.6 (6)
Cl-Mo-Cl′	137.8 (1)	P-C(1)-C(1)′	129.6 (8)
-P	89.0 (1)	Mo(2)-Mo(2)′-Cl	111.8 (5)
-P′	86.1 (1)	-P	91.9 (4)
P-Mo-P′	166.2 (1)	Mo-Mo(2)-Mo′	91 (1)
Mo-P-C(1)	114.7 (4)	Cl-Mo(2)-Cl′	136.4 (9)
-C(2)	111.6 (5)	-P	86.5 (2)
-C(3)	120.1 (5)	-P′	92.0 (2)
C(1)-P-C(2)	102.5 (9)	P-Mo(2)-P′	176.1 (9)

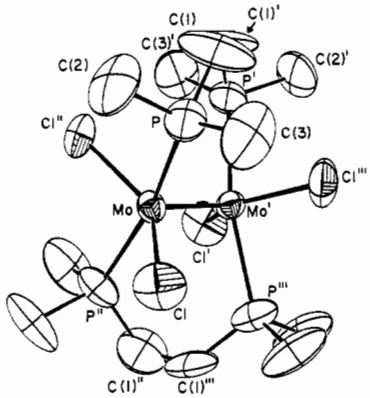

Figure 1. ORTEP view of the complete molecular geometry of β'-$Mo_2Cl_4(dmpe)_2$ (**1**) at the 42% probability level. Primed atoms are related to unprimed atoms by a twofold axis that perpendicularly bisects the C(1)–C(1)′ and Mo–Mo′ bonds. Doubly primed atoms are related to unprimed atoms by a twofold axis that is coincident with the Mo–Mo′ bond. Triply primed atoms are related to unprimed atoms by a third twofold axis perpendicular to the other two.

procedures for geometric and intensity measurements have been fully described elsewhere.[7] Pertinent crystallographic parameters are summarized in Table I, and details of the data collection, empirical absorption corrections,[8] and computational procedures[9] are available as supplementary material. Tables II and III list atomic positional parameters, while Tables IV and V give bond distances and angles for structures **1** and **2**, respectively. Complete tables of anisotropic thermal parameters and structure factors are included in the supplementary material. Figures 1 and 2 illustrate the structures and atom labeling schemes for the two complexes.

Spectral Measurements. The electronic absorption spectra of all $Mo_2X_4(LL)_2$ compounds discussed herein were obtained on Nujol mulls with use of a Cary 17D spectrophotometer. Solid samples (single crystals in some instances) were used to ensure that the twist angle (χ), which is capable of changing in solution, remained invariant so that meaningful comparisons could be made between spectral and crystallographic results.

Results and Discussion

Structures. Compound 1. β'-$Mo_2Cl_4(dmpe)_2$ adopts a structure (see Figure 1) quite similar to that reported for β-$Mo_2Cl_4(dmpe)_2$, except that the previously characterized compound possesses crystallographic C_2 symmetry (and idealized D_2 symmetry) while the new form has crystallographic D_2 symmetry with one twofold axis coincident with the Mo–Mo axis and two other twofold axes perpendicular to the Mo–Mo axis. There are two forms of disorder present in the structure. First, there is a secondary orientation of the Mo–Mo unit (with an occupancy of 4%) perpendicular to the major orientation. This type of disorder is very common in M_2X_8 species and was observed to a greater extent (8%) in the previous form of β-$Mo_2Cl_4(dmpe)_2$. Second, the abnormally short bond distance (1.21 (3) Å) between the carbon atoms of the ethylene group in the dmpe ligand indicates that the refined position of atom C(1) is an average of two disordered positions. This type of disorder has been observed before in complexes containing dmpe.[10] From the view in Figure 1, it is clear that atom C(1) is elongated in a direction approximately perpendicular to the C(1)–C(1)′ bond. A normal carbon–carbon single-bond distance of 1.54 Å would result if atom C(1) were displaced 0.47 Å in a direction perpendicular to the C(1)–C(1)′ bond. This amount of displacement is consistent with the root-mean-square amplitudes of thermal vibration (0.180, 0.432, 0.613 Å) for atom C(1). Refinement of a disorder model consisting of two half-atoms occupying positions at opposite ends of the elongation resulted

Table V. Bond Distances (Å) and Angles (deg) for β-$Mo_2Br_4(dmpe)_2$ (2)

	Distances		
Mo(1)-Mo(2)	2.169 (2)	P(2)-C(21)	1.85 (2)
-Br(1)	2.543 (2)	-C(22)	1.84 (2)
-Br(2)	2.547 (2)	-C(23)	1.84 (2)
-P(1)	2.538 (4)	P(3)-C(31)	1.85 (2)
-P(2)	2.534 (5)	-C(32)	1.85 (2)
Mo(2)-Br(3)	2.543 (2)	-C(33)	1.83 (2)
-Br(4)	2.554 (2)	P(4)-C(41)	1.88 (3)
-P(3)	2.547 (5)	-C(42)	1.84 (2)
-P(4)	2.544 (5)	-C(43)	1.85 (2)
P(1)-C(11)	1.84 (2)	C(11)-C(31)	1.56 (2)
-C(12)	1.84 (2)	C(21)-C(41)	1.54 (4)
-C(13)	1.88 (2)		
	Angles		
Mo(2)-Mo(1)-Br(1)	108.71 (8)	C(11)-P(1)-C(13)	102.6 (8)
-Br(2)	109.11 (8)	C(12)-P(1)-C(13)	106.0 (9)
-P(1)	101.9 (1)	Mo(1)-P(2)-C(21)	118.6 (7)
-P(2)	101.4 (2)	-C(22)	117.9 (7)
Br(1)-Mo(1)-Br(2)	142.18 (9)	-C(23)	109.6 (8)
-P(1)	85.9 (1)	C(21)-P(2)-C(22)	104 (1)
-P(2)	86.1 (1)	-C(23)	101 (1)
Br(2)-Mo(1)-P(1)	86.4 (1)	C(22)-P(2)-C(23)	103 (1)
-P(2)	86.6 (1)	Mo(2)-P(3)-C(31)	118.4 (6)
P(1)-Mo(1)-P(2)	156.7 (2)	-C(32)	118.8 (7)
Mo(1)-Mo(2)-Br(3)	107.62 (7)	Mo(2)-P(3)-C(33)	111.5 (7)
-Br(4)	108.95 (8)	C(31)-P(3)-C(32)	103.3 (9)
-P(3)	101.2 (1)	-C(33)	100.6 (9)
-P(4)	101.0 (2)	C(32)-P(3)-C(33)	102 (1)
Br(3)-Mo(2)-Br(4)	143.43 (9)	Mo(2)-P(4)-C(41)	120 (1)
-P(3)	85.9 (1)	-C(42)	118.0 (6)
-P(4)	86.6 (1)	-C(43)	110 (1)
Br(4)-Mo(2)-P(3)	86.6 (1)	C(41)-P(4)-C(42)	101 (1)
-P(4)	86.9 (1)	-C(43)	102 (1)
P(3)-Mo(2)-P(4)	157.8 (2)	C(42)-P(4)-C(43)	104 (1)
Mo(1)-P(1)-C(11)	118.7 (6)	P(1)-C(11)-C(31)	113 (1)
-C(12)	111.3 (7)	P(2)-C(21)-C(41)	114 (2)
-C(13)	117.1 (6)	P(3)-C(31)-C(11)	111 (1)
C(11)-P(1)-C(12)	99.0 (9)	P(4)-C(41)-C(21)	112 (2)

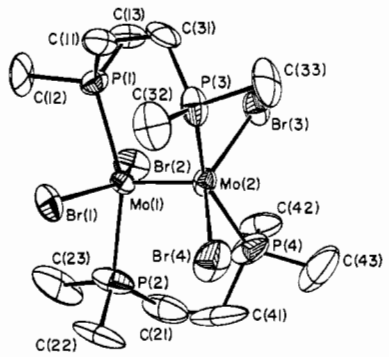

Figure 2. ORTEP view of the structure of β-$Mo_2Br_4(dmpe)_2$ (**2**). Ellipsoids are at the 50% probability level.

(7) Bino, A.; Cotton, F. A.; Fanwick, P. E. *Inorg. Chem.* **1979**, *18*, 3558.
(8) North, A. C. T.; Phillips, D. C.; Mathews, F. S. *Acta Crystallogr., Sect. A: Cryst. Phys., Diffr., Theor. Gen. Crystallogr.* **1968**, *24*, 351.
(9) Calculations were done with VAXSDP software on the VAX-11/780 computer at the Department of Chemistry, Texas A&M University.
(10) Cotton, F. A.; Falvello, L. R.; Najjar, R. C. *Inorg. Chem.* **1983**, *22*, 770.

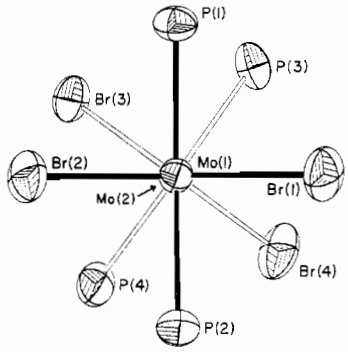

Figure 3. Central portion of the β-$Mo_2Br_4(dmpe)_2$ molecule viewed down the Mo–Mo axis.

in coalescence of the disordered pair. The large thermal parameters associated with the methyl carbon atoms, C(2) and C(3), are also indicative of the averaging of disorder.

Since the bridging dmpe ligands form six-membered rings with the Mo–Mo unit, this type of disorder corresponds to an interconversion between chair and boat conformations in these rings. This suggests that, contrary to the normal expectation, there is only a small energy difference between the chair and boat forms. It was previously shown that the chair conformation of the six-membered rings in β-$Mo_2X_4(R_2PCH_2CH_2PR_2)_2$ compounds is only slightly more stable than a twist conformation.[11]

It is noteworthy that the Cl–Mo–Mo–P torsional angle in β'-$Mo_2Cl_4(dmpe)_2$ is 33.8 (2)°, while the average such angle in β-$Mo_2Cl_4(dmpe)_2$ is 40.0 [1]°.[12] It has been shown[4,13] that the Mo–Mo bond distance in $Mo_2X_4(LL)_2$ compounds varies inversely with cos (2χ), where χ is the average internal torsional angle. The present results are in agreement with this since the Mo–Mo distance in β'-$Mo_2Cl_4(dmpe)_2$ is 2.168 (1) Å and that in β-$Mo_2Cl_4(dmpe)_2$ is 2.183 (3) Å.

A change in the amount of torsional twist should also result in different $\delta \rightarrow \delta^*$ transition energies for these two compounds (vide infra). One would expect the $\delta \rightarrow \delta^*$ transition in β'-$Mo_2Cl_4(dmpe)_2$ (**1**), which has the smaller χ value, to occur at higher energy than that in β-$Mo_2Cl_4(dmpe)_2$. This is the observed result, but the difference in the two transition energies (12.5 (1) $\times 10^3$ and 12.4 (1) $\times 10^3$ cm^{-1} for the β' and β cases, respectively) is within experimental error. It should be pointed out that these compounds fall on the "flat" portion of the curve in Figure 5, and thus a significant change in torsional angle is accompanied by a relatively small change in transition energy.

Compound 2. The structure of β-$Mo_2Br_4(dmpe)_2$ (see Figure 2) is, as expected, also similar to that of β-$Mo_2Cl_4(dmpe)_2$. Once again, the molecule has idealized D_2 symmetry, but in this case there is no crystallographic symmetry. Surprisingly, there is also no disorder of the Mo–Mo unit. The two six-membered rings formed by the dmpe ligands and the dimetal unit take on chair conformations. As Figure 3 illustrates, the rotational conformation of β-$Mo_2Br_4(dmpe)_2$ is staggered just as it is in β- and β'-$Mo_2Cl_4(dmpe)_2$. The average torsional angle about the Mo–Mo axis is 36.5 [3]°, and the Mo–Mo distance is 2.169 (2) Å. Thus, this compound also supports the observed dependence of Mo–Mo bond length on cos (2χ). Interestingly, the average torsional angle in β-$Mo_2Br_4(dmpe)_2$ is about halfway between the values of χ in the two forms of β-$Mo_2Cl_4(dmpe)_2$.

Dependence of the $\delta \rightarrow \delta^*$ Transition Energy on Torsional Angle. As noted above, the Mo–Mo bond length in $Mo_2X_4(LL)_2$ compounds has been used as a measure of δ-bond strength. Another convenient probe for the strength of the δ bond is the $\delta \rightarrow \delta^*$ transition energy, which falls in the visible region of the electronic

Table VI. $\delta \rightarrow \delta^*$ Transition Energies[a] and Torsional Angles (χ) for Structurally Characterized $Mo_2X_4(LL)_2$ Compounds

	compd	$\delta \rightarrow \delta^*$ transition ν, cm^{-1} $\times 10^{-3}$	χ, deg	cos (2χ)
A	$Mo_2Cl_4(dppm)_2 \cdot 2C_3H_6O$[b]	15.6 (1)	0.0	1.0
B	$Mo_2Br_4(dppm)_2 \cdot 2THF$[c]	15.3 (1)	0.0	1.0
C	$Mo_2Cl_4(tdpm)_2 \cdot 2CH_2Cl_2$[c]	14.5 (1)	20 [3]	0.77 (7)
D	$Mo_2Br_4(S,S\text{-dppb})_2$[d]	13.1 (1)	21.7 [2][e]	0.726 [5][e]
E	$Mo_2Cl_4(S,S\text{-dppb})_2$[d]	13.5 (1)	24.6 [12]	0.65 (3)
F	$Mo_2Br_4(arphos)_2$[f]	12.3 (1)	30.3 [3]	0.491 (9)
G	β-$Mo_2Cl_4(dppe)_2$[g]	12.8 (1)	30.5 [5]	0.48 (2)
H	β'-$Mo_2Cl_4(dmpe)_2$[h]	12.5 (1)	33.8 (2)	0.381 (6)
I	β-$Mo_2Br_4(dmpe)_2$[h]	11.8 (1)	36.5 [3]	0.292 (10)
J	β-$Mo_2Cl_4(dmpe)_2$[i]	12.4 (1)	40.0 [1]	0.174 (3)

[a] All spectra recorded as Nujol mulls. [b] Abbott, E. H.; Bose, K. S.; Cotton, F. A.; Hall, W. T.; Sekutowski, J. C. *Inorg. Chem.* **1978**, *17*, 3240. [c] Reference 13. [d] Agaskar, P.; Cotton, F. A., unpublished results. [e] Average of values for two independent dimers. [f] Cotton, F. A.; Fanwick, P. E.; Fitch, J. W.; Glicksman, H. D.; Walton, R. A. *J. Am. Chem. Soc.* **1979**, *101*, 1752. [g] Reference 11. [h] This paper. [i] Reference 4.

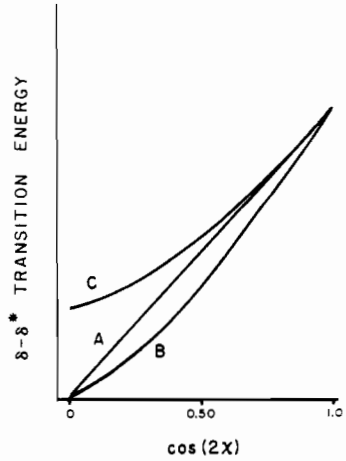

Figure 4. Schematic representations of the possible relationships between $\delta \rightarrow \delta^*$ transition energy and torsional angle (χ).

absorption spectra of these molybdenum dimers. Qualitatively, it is clear that as the twist angle, χ, increases, the energy of the $\delta \rightarrow \delta^*$ transition should decrease. However, the quantitative relationship to be expected between these two experimental quantities is not entirely a straightforward matter. For a one-electron case, $\sigma^2\pi^4\delta^2 \rightarrow \sigma^2\pi^4\delta\delta^*$ (or the equivalent $\sigma^2\pi^4\delta^2\delta^* \rightarrow \sigma^2\pi^4\delta\delta^{*2}$) we might expect the transition energy to be simply equal to the separation between the δ orbital and the δ^* orbital, $E(\delta^*) - E(\delta)$. The direct dependence of this separation on χ should be linear in cos (2χ), as is well-known. This is represented by line A in Figure 4. However, there is a secondary, or indirect, dependence of $E(\delta^*) - E(\delta)$ on χ due to the increase in the M–M bond length as χ increases; this will cause an additional decreasing trend in the δ overlap. However, this overlap and hence $E(\delta^*) - E(\delta)$ will still reach a value of zero only when cos (2χ) = 0 (χ = 45°) so long as the M–M distance remains finite. Thus, curve B (Figure 4), which is slightly concave upward, represents the sort of dependence of transition energy on twist angle to be expected for a genuine one-electron $\delta \rightarrow \delta^*$ transition. However, this is still an oversimplification, and we shall now turn to a discussion of the data that shows that, in fact, a curve of type C (Figure 4) is to be expected.

The energy difference between the two states, $^1A_{1g}$ and $^1A_{2u}$, arising from the $\sigma^2\pi^4\delta^2$ and $\sigma^2\pi^4\delta\delta^*$ configurations, is the sum of three contributions: (a) the orbital energy difference; (b) the interelectronic repulsion energies in the ground and excited states; (c) the electron correlation energy. In a simple Hartree–Fock–Roothan calculation, only (a) and (b) are included. This should also be the case for SW–Xα type calculations. The correlation

(11) Agaskar, P.; Cotton, F. A. *Inorg. Chem.* **1984**, *23*, 3383.
(12) Throughout this paper, a number in parentheses is an esd for a given individual value, while a number in brackets is equal to $[\sum_n \Delta_i^2/n(n-1)]^{1/2}$, where Δ_i is the deviation of the ith of n values from the arithmetic mean of the n values.
(13) Campbell, F. L.; Cotton, F. A.; Powell, G. L. *Inorg. Chem.* **1984**, *23*, 4222.

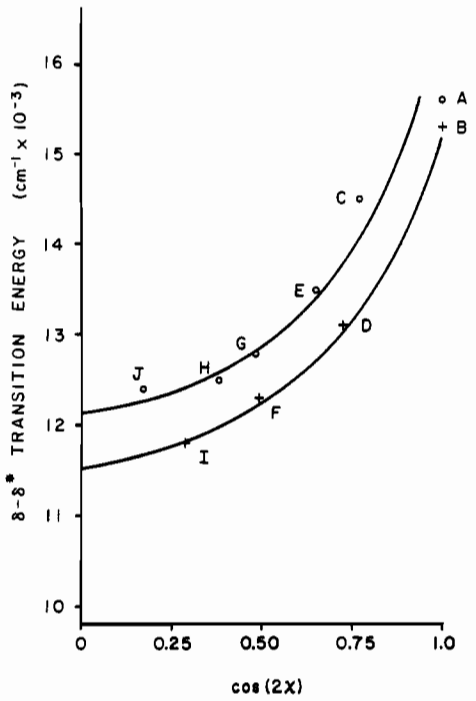

Figure 5. Plot of $\delta \rightarrow \delta^*$ transition energy vs. cos (2χ) for 10 $Mo_2X_4(LL)_2$ compounds (O, X = Cl; +, X = Br): A, $Mo_2Cl_4(dppm)_2 \cdot 2C_3H_6O$; B, $Mo_2Br_4(dppm)_2 \cdot 2THF$; C, $Mo_2Cl_4(tdpm)_2 \cdot 2CH_2Cl_2$; D, $Mo_2Br_4(S,S\text{-dppb})_2$; E, $Mo_2Cl_4(S,S\text{-dppb})_2$; F, $Mo_2Br_4(arphos)_2$; G, $\beta\text{-}Mo_2Cl_4(dppe)_2$; H, $\beta'\text{-}Mo_2Cl_4(dmpe)_2$; I, $\beta\text{-}Mo_2Br_4(dmpe)_2$; J, $\beta\text{-}Mo_2Cl_4(dmpe)_2$.

energy, which can be large in the case of weak bonds such as the δ bond, requires additional computation, usually by the method of configuration interaction.

Before a discussion of how this theoretical dissection of the total energy difference can be used to interpret the experimental results, it is important to state clearly what we are—*and are not*—doing when we extrapolate data for compounds with twist angles, χ, in the range $0 < \chi < 45°$ to $\chi = 45°$. For a molecule *actually* at 45° the exact degeneracy of the δ and δ^* orbitals makes the situation qualitatively different from that in the molecules we have studied. In all likelihood, a molecule with $\chi = 45°$ would be in a triplet ground state and the properties of this real molecule could not be predicted by a smooth extrapolation from the various singlet molecules now available for study. That is, indeed, not at all the purpose of the graphical extrapolation we shall next discuss. Our extrapolation will simply represent a way of deriving from experimental data *for singlet molecules* the energy of the $^1A_{1g} \rightarrow {}^1A_{2u}$ transition in the limit of a zero energy difference between the δ and δ^* orbitals *for singlet molecules*.

In Figure 5 we show a plot of all the measured $^1A_{1g} \rightarrow {}^1A_{2u}$ transition energies (with the approximation of using peak maxima rather than 0–0 vibronic energies) vs. cos (2χ). It would appear that the chloro and bromo compounds give quite separate curves, with a roughly constant energy difference of about 600 cm^{-1}. Since there must undoubtedly be interactions between the halogen $p\pi$ and $d\pi$ orbitals and the δ and δ^* orbitals, and these will differ for Cl and Br, the existence of a difference between the two classes of compounds is not surprising. However, we shall not attempt to account for the exact difference observed.

The major feature of significance in Figure 5 is that the curves can be extrapolated to a transition energy of about 11.8×10^3 cm^{-1} at $\chi = 45°$ (cos $(2\chi) = 0$), rather than to zero, as in Figure 4. What does this nonzero extrapolated value mean? At the extrapolated χ value of 45°, the orbital energy difference should be zero. Therefore, the energy of 11.8×10^3 cm^{-1} must correspond to differences in electron repulsion energy and correlation energy for the two states.

If we first assume (which may not be entirely justified) that electron repulsion energy and correlation energies are not dependent on cos (2χ) over the range 0.25–1.00, we may then compare this result with some calculations that have been done on the $Mo_2Cl_8^{4-}$ ion.[14] A calculation that took no account of electron correlation effects gave a transition energy of 9.2×10^3 cm^{-1} whereas the band in $Mo_2Cl_8^{4-}$ is actually observed at 18.8×10^3 cm^{-1}. The difference, 9.6×10^3 cm^{-1}, should then be due to the correlation effects. Comparing this number with the extrapolated energy in Figure 5, we could perhaps infer that there is some change in the electron repulsion energies or the correlation energy or both between the case of $Mo_2Cl_8^{4-}$ at $\chi = 0°$ and the $Mo_2X_4(LL)_2$ molecules at χ (extrapolated) = 45°. Clearly, however, the extrapolated energy in Figure 5 is an approximate measure of the electron correlation energies for the δ bonds in this class of molecules, and it has been obtained without recourse to any numerical quantum-mechanical theory. In a calculation[14] designed to include at least a major part of the correlation energy for the $Mo_2Cl_8^{4-}$ ion, the $^1A_{1g} \rightarrow {}^1A_{2u}$ transition was calculated to be at 15.2×10^3 cm^{-1}, thus placing a lower limit of 6.0×10^3 cm^{-1} on that energy. In this respect it is important to emphasize that for the one-electron case afforded by the $Tc_2Cl_8^{3-}$ ion, the transition energy can be calculated accurately without introducing any correction for correlation energy.

It would appear that the entire body of observations we have now assembled on $\beta\text{-}Mo_2X_4(LL)_2$ compounds is in excellent accord, qualitatively and even semiquantitatively, with theoretical expectations for the behavior of metal–metal δ bonds.

Acknowledgment. We thank the National Science Foundation for generous financial support.

Registry No. 1, 85115-86-2; 2, 94089-94-8; Mo, 7439-98-7; $Mo_2Cl_4(dppm)_2$, 64508-35-6; $Mo_2Br_4(dppm)_2$, 64508-34-5; $Mo_2Br_4(S,S\text{-dppb})_2$, 94089-95-9; $Mo_2Cl_4(S,S\text{-dppb})_2$, 88968-76-7; $Mo_2Br_4(arphos)_2$, 94089-96-0; $\beta\text{-}Mo_2Cl_4(dppe)_2$, 64508-32-3.

Supplementary Material Available: Details of the data collection and structure solution and refinement for compounds 1 and 2 and listings of anisotropic thermal parameters and structure factors (18 pages). Ordering information is given on any current masthead page.

(14) Noodleman, L.; Norman, J. G., Sr. *J. Chem. Phys.* **1979**, *70*, 4903.